




Article

Targeted Expression of TGFBIp Peptides in Mouse and Human Tissue by MALDI-Mass Spectrometry Imaging

Venkatraman Anandalakshmi ^{1,†}, Guillaume Hochart ^{2,†}, David Bonnel ², Jonathan Stauber ², Shigeto Shimmura ³ , Rajamani Lakshminarayanan ^{1,4} , Konstantin Pervushin ⁵ and Jodhbir S. Mehta ^{1,4,6,*} 

- ¹ Singapore Eye Research Institute, The Academia, 20 College Road, Level 6 Discovery Tower, Singapore 169856, Singapore; venk0020@e.ntu.edu.sg (V.A.); lakshminarayanan.rajamani@seri.com.sg (R.L.)
 - ² Imabiotech, Parc Eurasanté, 152 Rue Du Docteur Yersin, 59120 Loos, France; hochart.guillaume@imabiotech.com (G.H.); bonnel.david@imabiotech.com (D.B.); stauber.jonathan@imabiotech.com (J.S.)
 - ³ Department of Ophthalmology, Keio University, 35 Shinanomachi, Tokyo 160-8582, Japan; shige@z8.keio.jp
 - ⁴ Ophthalmology and Visual Sciences Academic Clinical Program, Duke-NUS Graduate Medical School, Singapore 169857, Singapore
 - ⁵ School of Biological Sciences, Nanyang Technological University, Singapore 637551, Singapore; kpervushin@ntu.edu.sg
 - ⁶ Singapore National Eye Centre, 11 Third Hospital Avenue, Singapore 168751, Singapore
- * Correspondence: jodhmehta@gmail.com; Fax: +65-6225-2568
- † Both authors (VA and GH) contributed equally towards the publication.



Citation: Anandalakshmi, V.; Hochart, G.; Bonnel, D.; Stauber, J.; Shimmura, S.; Lakshminarayanan, R.; Pervushin, K.; Mehta, J.S. Targeted Expression of TGFBIp Peptides in Mouse and Human Tissue by MALDI-Mass Spectrometry Imaging. *Separations* **2021**, *8*, 97. <https://doi.org/10.3390/separations8070097>

Academic Editor: Victoria Samanidou

Received: 10 May 2021

Accepted: 29 June 2021

Published: 3 July 2021

Publisher's Note: MDPI stays neutral with regard to jurisdictional claims in published maps and institutional affiliations.



Copyright: © 2021 by the authors. Licensee MDPI, Basel, Switzerland. This article is an open access article distributed under the terms and conditions of the Creative Commons Attribution (CC BY) license (<https://creativecommons.org/licenses/by/4.0/>).

Abstract: Stromal corneal dystrophies are a group of hereditary disorders caused by mutations in the *TGFBI* gene. The mutant TGFBIp is prone to protein aggregation and the mutant protein gets deposited in the cornea, leading to severe visual impairment. The mutations lead to a corneal specific protein aggregation suggesting the involvement of tissue-specific factors. The exact molecular mechanism of the process of tissue-specific protein aggregation remains to be elucidated. Differential proteolysis of mutant TGFBIp is a critical component of the disease pathology. The differential proteolysis gives rise to shorter peptides that are highly aggregation-prone and initiate the aggregation cascade. Analyzing the proteolytic processing of the different TGFBIp mutant may provide insight to aid in understanding the amyloid aggregation mechanism. We developed a MALDI-MSI methodology to identify expression and spatial localization of TGFBIp peptides in the cornea. Corneal tissue samples were collected from both control and dystrophic patients (with 2 different mutations), embedded in OCT and sectioned. The sections were trypsin digested and subjected to mass spectrometry imaging using a targeted approach to detect TGFBIp. MALDI-MSI identified peptides from TGFBIp that co-localized with the amyloid corneal deposits. In addition to the relative abundance data, the specific location of the peptides across the corneal sections as molecular signatures was also identified. Spatial distribution and intensity of the TGFBIp peptides showed differences between diseased and control models but also between the two LCD phenotypes. The TGFBIp peptide with m/z of 787.474 and m/z of 1179.579 showed increased expression in both LCD mutants compared to the controls. The peptide with m/z of 929.5 showed increased expression in the LCD phenotype with H626R mutation while the peptide with m/z of 1315.802 was abundant in the sample with R124C mutation. This initial report of 2D spatial protein signature and localization of TGFBIp may be expanded to other mutations to understand the proteolytic patterns of TGFBIp in different mutations.

Keywords: amyloid fibrils; cornea; lattice corneal dystrophy; matrix-assisted laser desorption ionization (MALDI); mass spectrometry imaging (MSI); TGFBIp

1. Introduction

The cornea is the clear avascular layer that forms the anterior part of the human eye [1]. The cornea is responsible for focusing light from objects onto the optical center of the human retina. The cornea also functions to prevent oxidative damage of internal tissues

caused by UV rays from the sun [2]. The adult human cornea is made up of five different layers namely: epithelium, Bowman's membrane, stroma, Descemet's membrane and the endothelium. Corneal transparency should be always maintained to have a normal clear vision. The stromal layer of the cornea is an extracellular matrix (ECM) rich in collagen and is the thickest layer of the cornea. The arrangement of collagen fibrils in the cornea plays an important role in maintaining the optical and biomechanical properties of the cornea [3].

The cornea is a protein-rich layer with about 609 proteins identified from the epithelium, stroma and endothelium [4]. The identification of unique proteins in the different layers of the cornea is important to understand the molecular mechanism of diseases associated with a specific protein and a specific region of the cornea [4]. The relative abundance or depletion of unique proteins has been associated with a number of ocular diseases that may serve as biomarkers to study disease progression and treatment [5–9]. Identification of a protein modification or its interacting partners and the exact location of a protein during a disease condition can provide us with more information on the disease pathway and the possibility of new treatment options.

Corneal dystrophies (CD) are a group of genetic disorders that are bilateral and affect visual acuity by increasing corneal opacification [10,11]. There are different types of corneal dystrophies based on the layer of the cornea affected. Genetic mutations have been associated and correlated with clinical phenotypes in some forms of CD. Mutations in transforming growth factor β -induced (*TGFBI*) gene are found to be associated with CDs affecting Bowman's membrane and the stromal region of the cornea [12]. Transforming growth factor β -induced protein (TGFBIP), also known as Keratoepithelin or BIGH3/ β IGH3, is an extracellular matrix (ECM) protein and the second most abundant protein in the human cornea [4,13,14]. The mutant protein is highly prone to aggregation and is proteolytically processed differently compared to the wild type (WT) protein that may lead to protein aggregation and deposition in the cornea [15,16].

TGFBIP is a 683 amino acid long protein and has a cysteine-rich domain, 4 Fasciclin like domains (FAS-1) and an RGD (Arg-Gly-Asp) signal domain [12,17–19]. There have been 74 different mutations reported in the *TGFBI* gene [20] and nearly 80% of the reported mutations/amino acid changes are present in the fourth FAS-1 domain of the protein. The age of onset of the disease, the type of protein deposition (amyloid fibrils, amorphous aggregates and combined forms), the severity of the clinical disease presentation and the layer of the cornea affected are dependent on the type of mutation [21]. Several proteomics studies have also identified TGFBIP to be the most abundant protein in amyloid corneal deposits of dystrophic patients [22–27]. Studying TGFBIP in greater detail with regards to its role in protein aggregation, deposition and its interaction with other aggregation-prone proteins may provide more information in understanding the pathology of CDs and treatment options to prevent protein aggregation.

There are several techniques used for the detection, quantification and localization of proteins [28,29]. The commonly used techniques are ELISA, co-Immunoprecipitation, western blot and immunohistochemistry where an antibody against the protein of interest provides information on the interacting partners of the protein, protein modification and anatomical location of the protein in the tissue sections. The main problem with these techniques is the availability of extremely sensitive and specific antibodies that can detect the protein of interest or its interacting partner. Another major issue faced by these techniques is the limited amount of sample or tissue available to perform all experiments. Protein profiling and quantification using a small amount of tissue became possible by using sophisticated mass spectrometric approaches. Proteomics studies using LC-MS/MS have become a particularly useful tool to study the proteolytic composition of tissues and protein modifications. The major constraints faced in the proteomics-based approach is the intricate sample preparation procedures, and its ability to list a relative abundance of proteins in samples, but not their anatomical localization in the tissue.

Matrix-assisted laser desorption/ionization (MALDI) Mass Spectrometry Imaging (MSI) is an advanced tool that combines both proteomics approaches and molecular

imaging modalities to provide information on the protein localization in tissue samples [30]. Many molecular images of the tissue sections can be directly generated without the need for a reagent specific to identify the target. MALDI-MSI has the advantage of using only a few tissue sections compared to other techniques with minimal sample preparation steps. Thus, this technique can be successfully used to identify potential biomarkers in disease diagnosis or study disease progression and evaluate tissue response to clinical treatment [31,32]. There are few reports of its use with ophthalmic tissue. Our group has used MALDI-MSI and reported the relative abundance of key proteins like TGFBIp, Apolipoprotein A-I, Apolipoprotein A-IV, Apolipoprotein E, Kaliocin-1, Pyruvate Kinase and Ras related protein Rab-10 in the corneal amyloid deposits of dystrophy patients compared to the controls [33]. Here we report the MALDI-MSI method development to identify TGFBIp in mouse and human corneal samples that are related to stromal CDs and their localization in healthy controls and diseased cornea.

2. Materials and Methods

2.1. Details on the Mouse and Human Samples

Control mouse corneal tissues (n = 1) were collected from WT C57BL/6 strains and used for the study. Diseased mouse cornea (n = 4) (GCD2/R124H) was a donation from Dr. Shigeto Shimmura, Keio University [34]. Human corneal samples as reported in our previous study [33] were collected from two patients with LCD (*TGFBI* mutations H626R [n = 1, male, age = 45] and R124C [n = 1, female, age = 62]) who were undergoing corneal transplantation at the Singapore National Eye Centre. Written informed consent was obtained from all patients prior to surgery. Transplant-grade Control tissue [n = 1, male, age = 54] from healthy control was obtained from Lion's Eye Institute, Tampa, USA. The study was conducted in accordance with the Declaration of Helsinki, and the ethical approval for the collection of the patient cornea was approved by the Singhealth Institutional Review Board.

2.2. Chemicals and Reagents

All chemicals including 2,5-Dihydroxybenzoic acid (DHB) matrix, α -Cyano-4- hydroxycinnamic acid matrix (CHCA), hematoxylin, eosin, chloroform, acetic acid, and LC-MS grade methanol and water, trifluoroacetic acid (TFA) and ammonium sulfate, were purchased from Sigma-Aldrich (St. Louis, MO, USA). Congo Red, Tissue Tek[®] OCT, Superfrost slides, and ethanol were purchased from VWR (Fontenay-sous-Bois, Paris, France). Porcine trypsin was purchased from Promega (Charbonnières-les-Bains, Lyon, France). Indium-tin-oxide (ITO) coated glass slides were purchased from Delta Technologies (Loveland, CO, USA). Mouse Recombinant TGFBIp and Human Recombinant TGFBIp (Transforming Growth Factor-Beta-Induced Protein ig-h3) standards were, respectively, purchased from Creative Biomart (Shirley, NY, USA) and Abcam (Paris, France).

2.3. Sample Preparation

Sectioning of the Cornea

The mouse corneas were embedded in Tissue Tek[®] Optimal Cutting Temperature (OCT) in a two-step protocol. Firstly, the flattest surface of the frozen cornea was laid onto a flat surface of solidified OCT in the cryostat chamber (−21 °C). Secondly, liquid OCT was quickly added on the top of the cornea to cover the entire surface and frozen as an OCT cube.

The OCT embedded sample was trimmed down until getting the first sections of the corneas at −35 °C with a cryo-microtome (Microm HM560, Thermo Scientific, Brignais, France). Quick H&E staining was performed to check the integrity and morphology of the sections before collecting 10 μ m-thick sections for analysis. These sections were mounted on ITO glass slides, cryodesiccated for 1 h then dried under vacuum in a desiccator for 20 min before further use. Low-resolution optical images of each slide were acquired using a standard office type scanner (Hewlett-Packard, Palo Alto, CA, USA). Additional

serial sections were prepared on Superfrost slides for staining with Hematoxylin and Eosin. Congo red staining was added in the case of human corneas. Human corneas were simply fixed on OCT and sectioned according to the procedure described above.

2.4. Washing of the Sections

A six-step washing was applied to the tissue sections on the ITO slides in order to enhance protein detection [35]: 70% Ethanol for 30 s/100% Ethanol for 30 s followed by Carnoy's solution (60% Ethanol/30% chloroform/10% acetic acid 1:1:1 *v/v/v*) for 2 min/100% Ethanol for 30 s/Water for 30 s/100% Ethanol for 30 s.

2.5. Digestion

In order to detect characteristic peptides from different proteins, the automatic device SunCollect (Sunchrom, Friedrichsdorf, Germany) was used to spray porcine trypsin at 40 µg/mL in 50 mM ammonium bicarbonate onto the tissue sections and standard samples. Fifteen cycles of trypsin sprayed at room temperature and 10 µL/min flow rate were performed on the entire ITO slide prior to its incubation at 37 °C in a hermetic box overnight and further dried under vacuum for 15 min before matrix deposit.

Positive control of the digestion in solution was prepared with a 10 µM working solution of the TGFBIp (human or mouse) mixed with the enzymatic solution in 1:1 *v/v*.

2.6. MALDI Matrix Deposit

MALDI matrices (DHB 40 mg/mL in Methanol: Water + 1%TFA 1:1 *v/v*) and MALDI matrix (CHCA 10 mg/mL, Acetonitrile/0.2%TFA, 125 mM and Ammonium Sulfate 7:3 (*v/v*)) were sprayed on the tissue sections using the automatic device SunCollect or the TM Sprayer device (HTX Imaging, Chapel Hill, NC, USA). Six layers of the enzyme were sprayed at 10 µL/min following Suncollect parameters: Speed X = 1, Speed Y = 1 and Z position = 35).

Matrix deposit sprayed with automatic devices is crucial to have homogenous layers on the tissue sections and best in situ extractions without delocalization of targeted analytes.

Based on optimized methods for both automated Suncollect and HTX instruments, complementary results were obtained with regards to the composition of the matrices. Although the coating was very homogenous for DHB and CHCA, acetonitrile or methanol organic contents in the matrix with or without salts (e.g., ammonium sulfate) definitely provided extraction differences for the peptides.

These two complementary matrices demonstrated that TGFBIp could be followed in human tissue based on a series of peptides after TGFBIp digestion.

2.7. Congo Red and Hematoxylin and Eosin

For WT mouse corneal sections, there was first a verification of the histology to validate the section plane then imaging of a serial section with H&E staining was also performed after MSI analysis.

Presence of corneal amyloid protein deposits from the clinical samples (patients) was visualized with Congo red staining on serial sections followed by mounting the slide with aqueous medium Aquatex® and drying before High-definition scanning ×20 with a HD Panoramic 250 Flash 2 scanner (3H Histech, Budapest, Hungary).

2.8. MALDI-FTICR Acquisitions and Data Analysis

Mass Spectrometry Method

MALDI Mass Spectrometry Imaging (MSI) of the mouse and human corneas were performed at high spatial resolution (20 µm) using a 7T-MALDI-FTICR (Solarix, Bruker Daltonics, Bremen, Germany) with a Smartbeam II laser in minimum mode with a repetition rate of 2000 Hz. MALDI-FTICR calibration was first set up with a Pepmix calibration standard (Bruker) in linear mode prior to online calibration with matrix peaks.

Collision-Induced-dissociation was based on a 10 Da mass window with collision energy at 26 V.

Full Scan positive modes within 300–2000 Da mass ranges were selected for imaging with online calibration using matrix peaks (mass accuracy < 3 ppm). The mass spectrum obtained for each position of the images corresponded to the averaged mass spectra of 300 consecutive laser shots on the same location. FTMS Control 2.0 and FlexImaging 4.1 software packages (Bruker Daltonics, Bremen, Germany) were used to control the mass spectrometer and set imaging parameters.

In silico peptide mass fingerprint (PMF) from TGFBIp was compared to experimental PMF from the working standard protein digest for both mouse and human TGFBIp recombinants.

Protein digests from the tissue sections were compared to the working standard digests to establish the list of positive matches followed by the fragmentation of these hits using MS/MS mode of the Solarix (qCID) for validation of the peptide sequences.

2.9. Software

Peptide identification was done using DataAnalysis 4.1, Biotoools 3.1, SequenceEditor3.1, SCiLS v 3.02.7804 software (Bruker daltonics, Bremen, Germany). Mass tolerance was established at 10 ppm maximum for all interrogations. Online databases Mascot (Swissprot database, human, variable modifications including Carbamidomethyl and Oxidation) and Blast (UniProtKB/SwissProt database in Protein Blast, humans (taxid: 9605)) were queried for peptide identifications. Up to two missed cleavages were allowed after digestion. Image treatment including optical, molecular images and overlays were realized with Multimaging software (ImaBiotech SAS, Loos, France).

2.10. Immunohistochemistry

Samples were fixed with neutral buffered 4% paraformaldehyde. After quenching with ice-cold 50 mM/L ammonium chloride (Sigma), samples were permeabilized with 0.15% saponin and blocking with 1% bovine serum albumin (Sigma) and 2% normal goat serum (Invitrogen), followed by incubation with primary TGFBI/BIGH3 antibodies (Catalogue number #, 60007-1, Proteintech) for 2 h at room temperature. The primary antibody is a mouse monoclonal antibody that is raised against residues 199–406 of human TGFBIp and recognizes both human and mouse TGFBIp. After PBS washes, they were labelled with appropriate Red X or Alexa488 conjugated IgG secondary antibody (Jackson ImmunoRes Lab, West Grove, PA, USA) and fluorescein-conjugated phalloidin (Invitrogen). After washes, samples were mounted with Fluoroshield with DAPI (4',6 diamidino 2 phenylindole; Santa Cruz Biotech, Santa Cruz, CA, USA) and viewed under fluorescence microscopy (AxioImager Z1, Carl Zeiss, Oberkochen, Germany).

3. Results

3.1. Evaluation by Microscopy and Histological Staining

The corneal slit lamp bio-microscopy images (Figure 1) from WT C57BL/6 mouse, diseased mouse (GCD2/R124H), and human cornea are shown. The images indicate that the cornea remained clear in both control human and WT mice. The images from corneal dystrophy patients with TGFBI-H626R and TGFBI-R124C mutations displayed corneal opacities from protein deposits in the cornea. The mutations in the patients were also verified by blood DNA sampling and sequencing. The integrity of the tissue was also verified by H&E staining for the human corneal tissue sections (Supplementary Figure S1). The staining showed that the tissue sections from both mouse and human remained intact. Additionally, congo red staining was done on the control mouse and patient corneal tissue sections to identify the amyloid protein deposits (Supplementary Figure S1). The protein deposits were identified by dark red/brown colored spots as indicated by arrows in the dystrophic patient samples. The sections obtained from a patient

with *TGFBI*-H626R mutations stained better with congo red dye compared to the patient with *TGFBI*-R124C mutation.

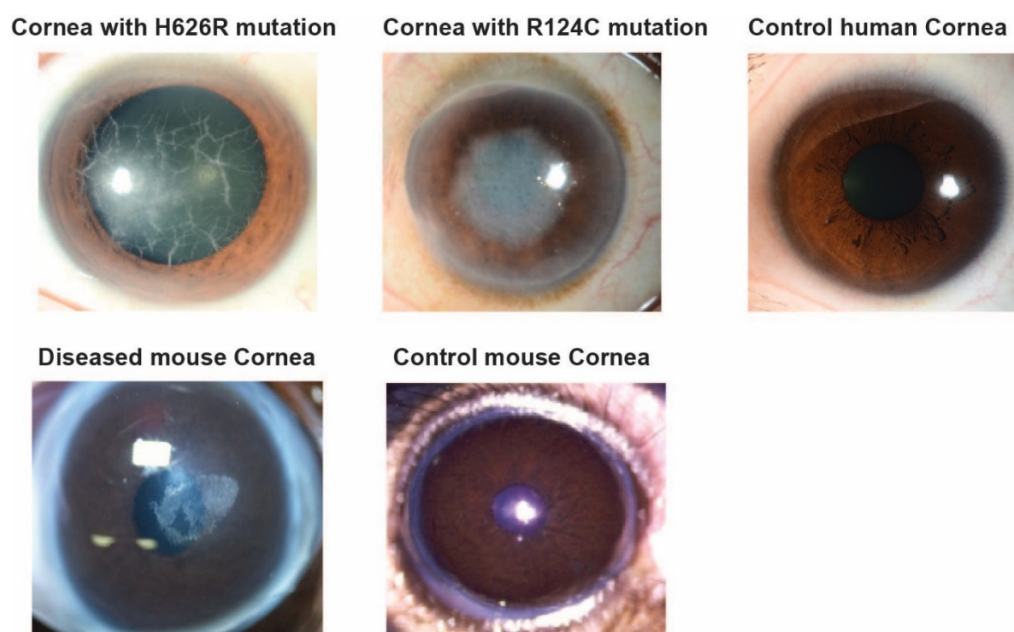


Figure 1. Corneal images showing lattice lines and aggregated proteins with opaque cornea in diseased mouse (GCD2/R124H) and dystrophic patients with H626R mutation and R124C mutation. Corneal images showing clear cornea for both the control human and control mouse samples.

3.2. Method Development to Detect *TGFBI*p in Control Mouse and Human Corneal Tissue

The control mouse corneal tissue was analyzed using the DHB matrix. The detailed workflow of the *TGFBI*p detection process is described in Figure 2.

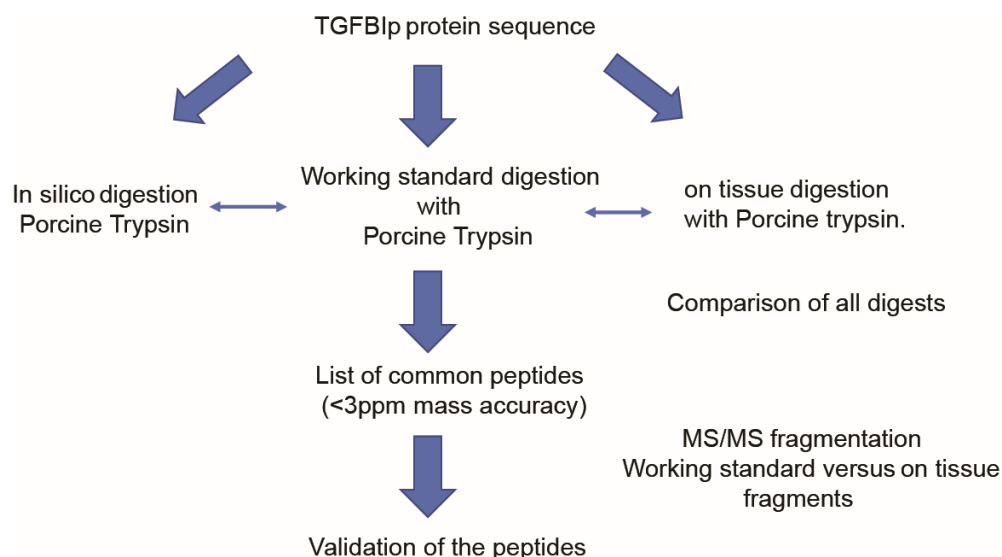


Figure 2. Process for method development to detect *TGFBI*p in the corneal samples (process chart).

PMFs (Peptide Mass Fingerprinting) were obtained in the control mouse sections after trypsin deposition (Figure 3A). The trypsin digest of standard *TGFBI*p spotted on control sections led to expected peptide peaks according to in silico prediction tools (Supplementary Table S1). There were about 21 peptides from the standard *TGFBI*p solution digest, matching with the in-silico digestion. However, these peptides were not observed after digestion of intact mouse corneal tissue.

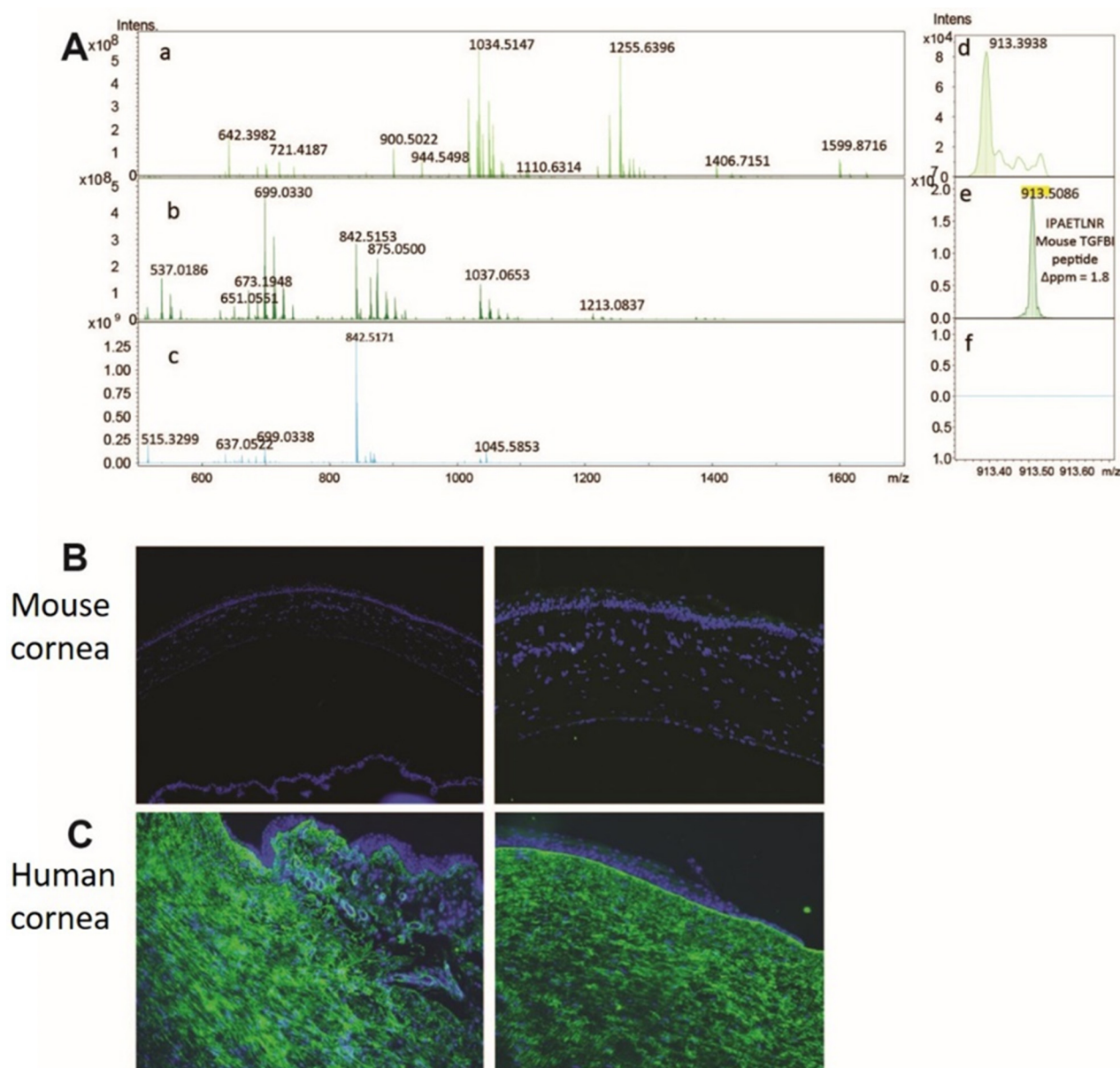


Figure 3. (A) (a–c): Peptide mass fingerprint spectra obtained in (a) Mouse cornea, (b) TGFBIp reference standard, (c) Control matrix with tryptic enzyme. (d–f): Corresponding zooms for one of the TGFBIp digests from the standard (m/z 913.5086). (B) Immunohistochemistry results of TGFBIp staining on WT-mouse cornea indicating absence or extremely low expression of TGFBIp. (C) Immunohistochemistry results of TGFBIp staining on WT-human cornea indicating abundant presence throughout the cornea. The blue (DAPI) color stain indicates the presence of nucleus, and the green color indicates the presence of TGFBIp protein.

Our immunohistochemistry analysis of mouse corneal TGFBIp suggested a very low expression of the protein in corneal tissue (Figure 3B) and the phenotypic expression of GCD2 TGFBI- corneal dystrophy mouse model was not very severe compared to the disease phenotype in humans. Hence, we decided to validate the TGFBIp expression in human corneas with stromal corneal dystrophy, as a next step. The human control corneal tissue was subjected to immunohistochemistry to detect the expression of TGFBIp (Figure 3C).

The analysis suggested a very high expression of the protein in control human corneas, TGFBIp is the second most abundant protein in the cornea [4]. With very high TGFBIp expression in human cornea, the human control and patient samples were subjected to MALDI-MSI to identify the anatomical location of TGFBIp in patient's corneal deposits.

3.3. Method Development to Detect TGFBIp in Human Samples

The human control and patient corneal tissue were subjected to overnight trypsin enzymatic digestion followed by the deposition of the DHB matrix and subjected to MALDI-MSI. The analysis of the peaks showed that two peptides matched with the in silico digestion of the human TGFBI, namely [ALPPRER] at m/z 838.489 and [SPYQLVLQHSR] at m/z 1327.712 with <3 ppm of mass accuracy for both control and patient tissue sections. The MALDI-FTICR spectrum of TGFBIp trypsin digests in solution were also matched with the in-silico digest, and a peptide list with 17 matches identified (Supplementary Figure S2). The implemented PMF in Mascot database also matched with the presence of TGFBI protein (Supplementary Figure S3) for the control and dystrophic corneal samples.

In order to validate the trypsin digest of TGFBIp, the peptide [ALPPRER] with m/z 838.489 was also subjected to fragmentation with qCID (quadrupole Collision Induced Dissociation) mode of the Solarix and allowed to retrieve the experimental fragments of the TGFBIp standard (Figure 4, Supplementary Figure S4).

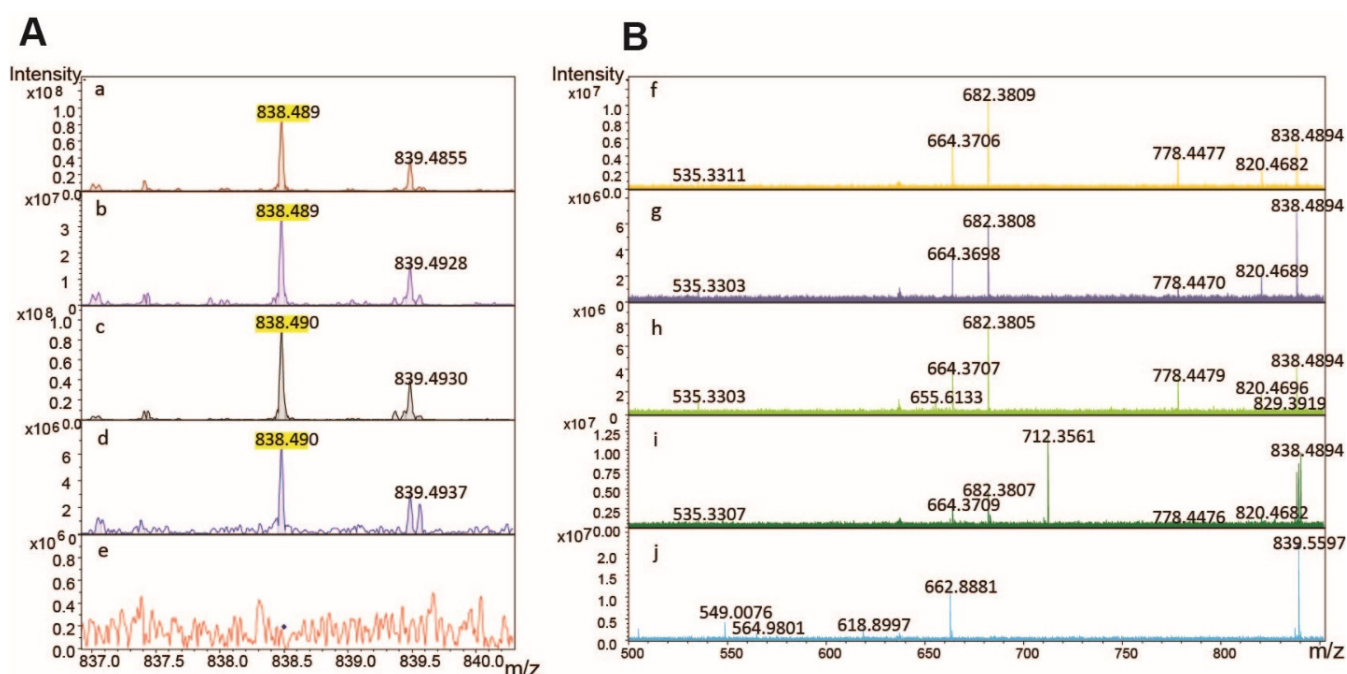


Figure 4. (A)(a–e): MALDI-FTICR MS spectra for the detection of the TGFBIp digest at m/z 838.489 (peptide sequence ALPPRER with accuracy >1 ppm) in (a) Wild type cornea, (b) Diseased cornea with H626R mutation, (c) Diseased cornea with R124C mutation, (d) TGFBIp reference standard, (e) Control matrix with tryptic enzyme. The peptide at m/z 838.4894 was detected in both diseased human corneas with H626R mutation and R124C mutation and wild type sample. No interfering peak was found in the control matrix with trypsin. (B)(f–j): MALDI-FTICR fragmentation spectra for the validation of the TGFBIp digest at m/z 838.489 (peptide sequence ALPPRER) in (f) Wild type cornea, (g) Diseased cornea with H626R mutation, (h) Diseased cornea with R124C mutation, (i) TGFBIp reference standard, (j) Control matrix with tryptic enzyme. Product ions at m/z 535.3307, m/z 664.3709, m/z 682.3807, m/z 712.3561, m/z 778.4476 and m/z 820.4682 were observed after fragmentation of the peptide ALPPRER in the human TGFBIp standard. These fragments were also detected after fragmentation of the m/z 838.4894 in both diseased human corneas #1 and #2 and in the wild type human cornea (except the fragment at m/z 712.3561 which was additionally found in TGFBIp reference standard).).

The fragmentation resulted in five product ions (m/z 535.330, m/z 664.370, m/z 682.380, m/z 778.447 and m/z 820.468) in TGFBIp standards and also in both dystrophic patient corneas (Figure 4Bf–i. Fragmentation of the peptide [ALPPRER] with m/z 838.489 in control human cornea resulted in five fragments (Figure 4B) with the absence of m/z 712.356, which was additionally found in TGFBIp reference standard. The peptide fragment with m/z 838.489 was also queried in the MASCOT server and the search resulted in TGFBIp as the predominant match (Supplementary Figure S4). The presence of TGFBIp was thus confirmed in the control as well the patient samples. The peptide with m/z 1327.712 could not be verified with fragmentation results, as the MS/MS spectrum did not match with the MS peak and hence was not included in the analysis.

Complementary results were obtained when the human tissue sections were coated with CHCA Ammonium Sulfate matrix leading to specific TGFBI peptides at m/z 787.474 [VIGTNRK], m/z 929.508 [IPSETLNR], m/z 1179.579 [DGTPPIDAHTR] and m/z 1315.802 [LTLLAPLNSVFK]. Out of the five peptides obtained as a result of trypsin digestion 3 peptides belong to the third and fourth FAS1 domain of TGFBIp. The m/z that was obtained matched with the TGFBIp sequence due to the high spectral resolution of FTICR. The peptide sequences were also subjected to BLAST analysis and all the peptides were found to be unique to TGFBIp (Supplementary Figure S5).

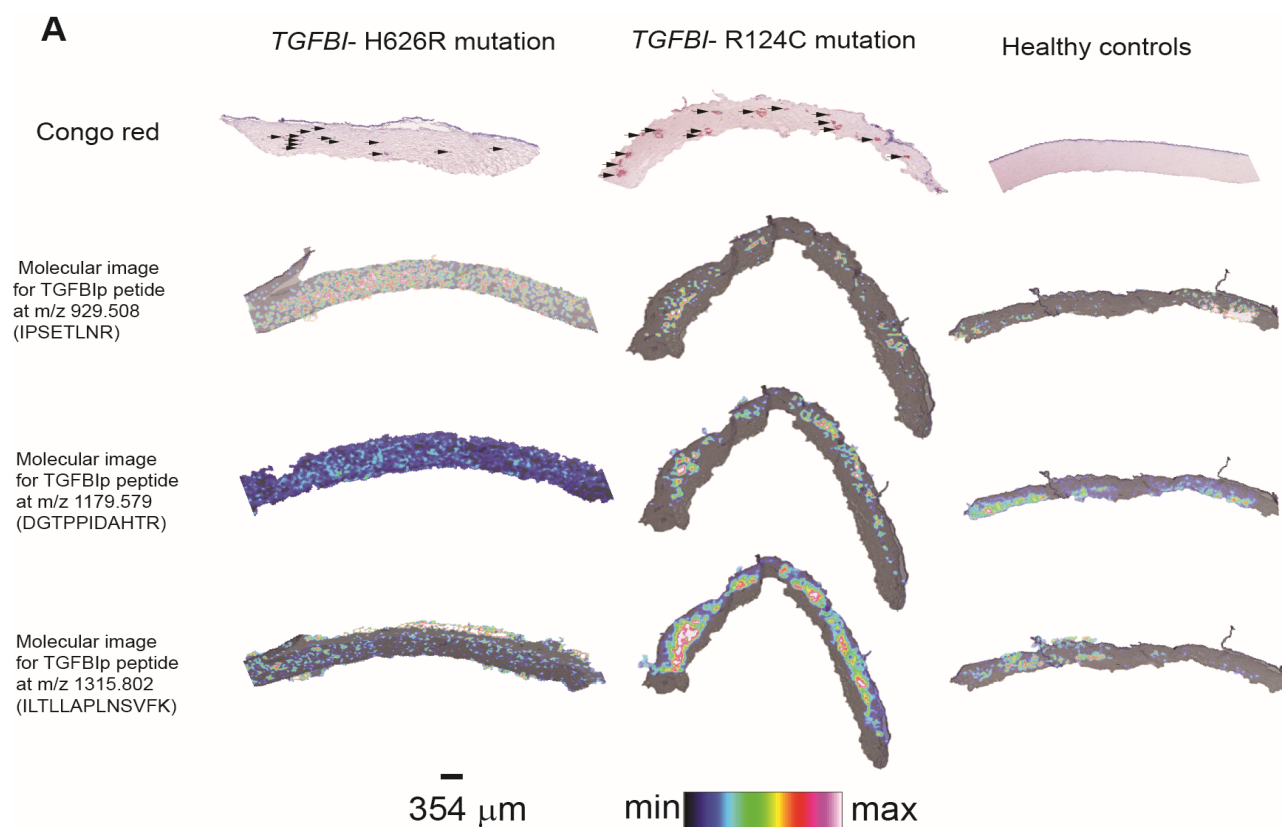


Figure 5. Cont.

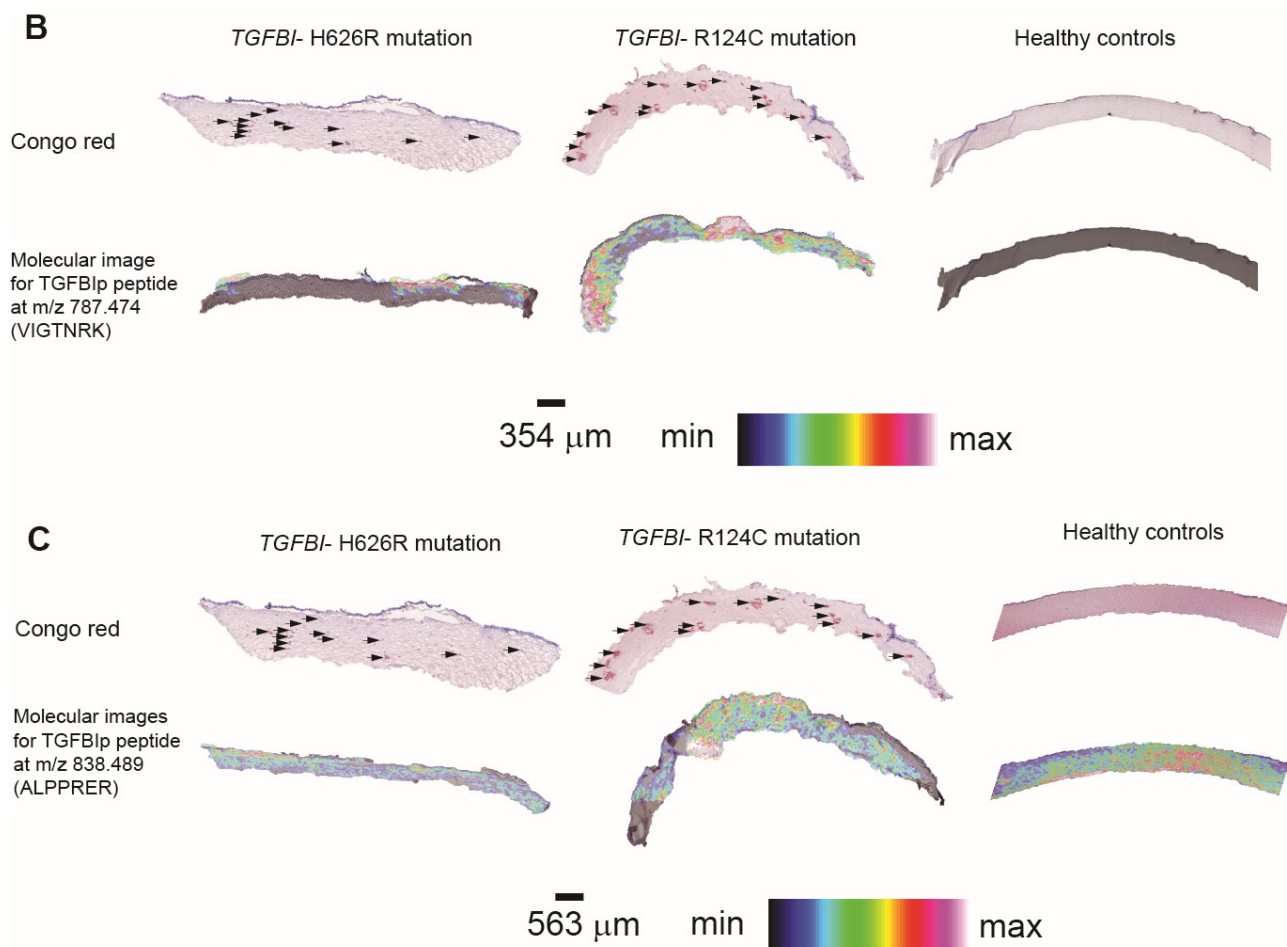


Figure 5. (A–C): MALDI-MSI Images showing the distribution of the five TGFB1p peptides in patient and donor control corneas. The congo red staining is also shown for the mutants and the control corneal tissue samples. The arrow marks in the congo red staining points the amyloid protein deposits in the patient. The patient with R124C mutation had more visible amyloid plaques than the patient with H626R mutation. The mass spectrometry imaging of most of the TGFB1p peptides colocalizes with the amyloid plaques in congo red staining indicating that mutant TGFB1p is the major component of the amyloid plaques. TGFB1p peptide is also found to be localized in other regions as TGFB1p is the second most abundant protein in the human cornea.

The MALDI-MSI images for the 5 *TGFB1* peptides were overlaid with the respective Congo red staining images for both the control and the dystrophic patients to visualize the distribution of these peptides on the tissue samples (Figure 5A–C). The MSI images of all five peptides co-localized very well with the Congo red staining representing the amyloid corneal deposits from dystrophic patients. This result suggested that TGFB1p is an integral component of the corneal deposits in the dystrophic patients which is in strong agreement with the LC-MS/MS quantification data of the composition of the amyloid deposits from dystrophic patients with the same R124 and H626R mutations reported here [25,33]. Some of the peptides had differential expression in some mutation compared to the control samples. The peptide with m/z 929.508 showed a higher distribution in the patient sample with *TGFB1*-H626R mutation compared to the control and *TGFB1*-R124C mutation. Similarly, the peptide with m/z 787.474 showed very high expression in the patient with *TGFB1*-R124C mutation compared to the patient with *TGFB1*-H626R mutation or healthy control samples. The expression of the peptide with m/z 838.489 was highly expressed in the control cornea compared to the two patient samples. These results suggest that each of the mutant protein undergo differential proteolysis based on the type of mutation. It has also been shown that the mutations cause a local structural change around the site of mutation in the protein and thereby cause increased/decreased access of the

protein to proteolytic enzymes that process the protein. In some mutations the increased access of proteins to proteolytic enzyme may result in shorter peptides that may act as aggregation seeds and trigger the process of amyloid fibril aggregation. In mutant proteins where there is a decreased access to proteolytic enzyme, the mutant protein may stay longer in the system with increased half-life and could not be cleared by the system. This may result in amorphous protein aggregates and the mutant protein may be deposited in the cornea due to incomplete clearance. Thus, understanding the proteolytic processing of TGFBIp in each type of mutation has become important to understand the turnover rate and processing of TGFBIp.

4. Discussion

The prevalence of TGFBIp associated corneal dystrophy has increased in recent times with more cases and new mutations being reported worldwide. This is due to the increased accessibility towards affordable genetic screening tools and increased awareness about the disease. Therefore, we have identified and optimized another technique to visualize TGFBIp localization and distribution in normal and dystrophic corneas by MALDI-MSI. This technique requires fewer sample sections and may be used to profile samples based on an exploratory proteomics approach. In our previous publication [33], we reported the first study to use MALDI-MSI on corneal tissue samples. We studied the untargeted expression and co-localization of several proteins with corneal amyloid deposits in patients with *TGFBI*-H626R and *TGFBI*-R124C mutations. We identified the presence of Apolipoprotein E, TGFBIp, Apolipoprotein-IV, Apolipoprotein A-I and Pyruvate kinase enriched in the amyloid corneal deposits in patients. In this paper, we report the localization of TGFBIp peptides, as this protein plays a major role in stromal corneal dystrophies. There are reported differences in the proteolytic processing of mutant TGFBIp based on the type or nature of the amino acid substitution also identified in our study [15,36–38].

We tried to detect the expression of TGFBIp and other proteins in the mouse samples but were unable to detect the TGFBIp peptides in the mouse model. There may have been several factors that contributed to the inadequate detection. Firstly, it is shown that there is differential expression of TGFBIp across species, and mice express significantly lower amount of TGFBIp in the cornea than humans, (more than ten folds less) [36]. The second reason might be due to the lack of sensitivity due to the matrix used for MALDI-MSI. For the mouse samples, only the DHB matrix was used for protein detection. Repeating the experiments with another kind of matrix like CHCA might have provided improved detection. The type of MALDI matrix used in the sample preparation and detection is an important step and is based on the type of target analyte to be studied. So, one type of matrix may not be suitable for all analytes or species and hence involves a trial-and-error method. Since we focused more on the human samples, we did not try other types of the matrix for the mouse samples. The third reason might be due to the nature and molecular function of the target protein: TGFBIp. It is known to bind to other ECM proteins, collagen and cell adhesion proteins. The on-tissue enzymatic digestion used in the experiments did not have reduction or alkylation steps to reduce the complex bonds and interactions between TGFBIp and other proteins. The porcine trypsin used in the protein digestion may not have had access to TGFBIp for enzymatic cleavage.

It has been previously reported that mutant TGFBIp undergoes a differential proteolysis compared to the WT protein [15,37,38] depending on the nature and site of mutation. The nature of amino acid substitution cause either increased or decreased stability of the mutant proteins that influence the overall turnover rate of the protein [37]. The site of mutations thus dictates the structural and proteolytic susceptibility of the mutant TGFBIp towards various proteolytic enzymes. In our study the samples were obtained from lattice dystrophy patients. Even for samples with the same clinical phenotype, we observed changes in the proteolytic patterns based on the position of the mutation and the type of amino acid substitution. When the imidazole ring containing Histidine, residue is replaced by a positively charged Arginine residue in the H626R mutation, the TGFBIp peptide

IPSETLNR with m/z 929.5 showed increased expression compared to the R124C and the control samples. Similarly, when the positively charged Arginine residue 124 is replaced by an uncharged cysteine residue in R124C mutation, the peptide LTLLAPLNSVFK with m/z of 1315.802 is highly expressed in the tissue compared to the H626R mutation and the control. For both the mutations there was increased expression of peptide VIGTNRK with m/z 787.474 while there was no expression of this peptide on the control sample. Mutations leading to the LCD phenotype may cause structural destabilization and increase access to proteolytic enzymes, thus causing an increase in protein turnover rates. Increased proteolysis in the LCD mutant proteins, may give rise to several amyloidogenic peptides that are capable of acting as amyloid seeds and initiating an amyloid aggregation cascade [26,33,37,38].

Studies have also shown that Granular Corneal Dystrophy (GCD) associated mutations, may result in increased structural stability of mutant TGFBIp [26,37,39]. The increased stability makes the mutant protein less susceptible to any proteolytic degradation in the cornea resulting in an increase turnover rate of mutant proteins which may turn into insoluble aggregates [37,40,41]. The proteolytic processing and turnover rate of mutant TGFBIp may be very important to understand the disease mechanism. In this study, we have reported that trypsin enzymatic fragments of mutant TGFBIp in two commonly occurring LCD mutations, and the anatomical localization of these peptides in the corneal tissue. There were differences in the trypsin digestion and expression of peptides from mutant TGFBIp compared to the controls. There were also differences observed in the localization of some peptides between the two LCD phenotypes compared to the healthy controls. The differential expression of these peptides needs to be verified with other samples with the same mutation across different ethnicities due to the differences observed in the phenotypic expression of the same mutation [41–44]. The differential peptide expression may play an important role in understanding mutation dependent protein processing mechanism, which have already been suggested by various previous publications [15,22–27,37,38].

The localization of tryptic peptides derived from other common LCD phenotypes compared with the peptides generated from GCD phenotypes may provide us with new insights in understanding the disease mechanism based on the patterns of peptide localization in each type of mutation. These peptide expression patterns in the corneal stroma may also provide insights if the extracellular environmental changes and/or which mutations in the protein are responsible for triggering the aggregation cascade, observed in stromal corneal dystrophies. The peptide processing and proteolysis may also be important to identify therapeutic compounds that may prevent the formation of amyloidogenic peptides and thus prevent protein aggregation and amyloid fibril formation. Hence, in this report, we were able to detect five peptides of interest from TGFBIp. We were also able to validate the differential protein processing patterns in the WT, compared to other mutant forms of the protein using a new methodology. The confidence level of such an experiment can be enhanced by optimization of methods on sample preparation and processing to detect more TGFBIp peptides and by validating other TGFBIp mutants.

Supplementary Materials: The following are available online at <https://www.mdpi.com/article/10.3390/separations8070097/s1>, A list of supplementary information is attached to the manuscript as follows: Supplementary Table S1: TGFBI mouse digests in solution matching in silico digestion. Supplementary Figure S1: H&E and Congo red staining for mouse, human samples Supplementary Figure S2: 7T-MALDI-FTICR spectrum of TGFBIp digest. Supplementary Figure S3: Search parameters used for TGFBIp to match PMF obtained from the control and treated tissue sections. Supplementary Figure S4: MS/MS fragmentation of m/z 838.489 in (a) Digested human cornea, (b) Control trypsin only and (c) Query of the MS/MS in Mascot database. Supplementary Figure S5: BLAST results of all the five peptides reported for TGFBIp.

Author Contributions: V.A., R.L., K.P., and J.S.M. were involved in the conceptualization of the study and to secure study funding. V.A. performed immunohistochemistry experiments and analysed data. G.H., D.B. and J.S. performed Mass Spectrometry Imaging experiments and analysed Mass Spectrometry Imaging data. S.S. supervised mouse experiments and analysed data. V.A., R.L., S.S. and G.H. were involved in the draft preparation of the original manuscript. All authors reviewed and edited the manuscript. All authors have read and agreed to the published version of the manuscript.

Funding: The authors would like to acknowledge the funding support from SNEC-HREF R1376/62/2016, SNEC-HREF R1429/12/2017 to JSM and SERI-Lee foundation pilot grant R1586/85/2018 (LF0618-4) to VA.

Institutional Review Board Statement: The study was conducted according to the guidelines of the Declaration of Helsinki, and approved by SingHealth Centralized Institutional Review Board (CIRB) Protocol number R978/87/2012.

Informed Consent Statement: Informed consent was obtained from all subjects involved in the study.

Data Availability Statement: The data presented in this study are available on request from the corresponding author.

Acknowledgments: The authors would like to acknowledge Assistant Prof Amutha Veluchamy Barathi Head, Translational Pre-Clinical Model Research Platform, Singapore Eye Research Institute for providing WT mouse cornea samples.

Conflicts of Interest: The authors of the manuscript declare no competing commercial/financial interests.

Abbreviation

α CHCA	α -Cyano-4-hydroxycinnamic acid
CD	Corneal Dystrophy
ECM	Extracellular matrix
FAS1	Fasciclin like Domain 1
GCD	Granular Corneal Dystrophy
ITO	Indium-tin-oxide
KDa	Kilodalton
LC	Liquid Chromatography
LCD	Lattice Corneal Dystrophy
MALDI	Matrix-assisted laser desorption/ionization
MS	Mass Spectrometry
MSI	Mass Spectrometry Imaging
PBS	Phosphate Buffered Saline
PMF	Peptide Mass Fingerprinting
qCID	Quadrupole Collision Induced Dissociation
TGFB1	Transforming Growth Factor Beta Induced gene
TGFB1p	Transforming Growth Factor Beta Induced protein
WT	Wild Type
3D	3 Dimensional

References

1. Hassell, J.R.; Birk, D.E. The molecular basis of corneal transparency. *Exp. Eye Res.* **2010**, *91*, 326–335. [[CrossRef](#)]
2. Land, M.F.; Fernald, R.D. The Evolution of Eyes. *Ann. Rev. Neurosci.* **1992**, *15*, 1–29. [[CrossRef](#)]
3. Jue, B.; Maurice, D.M. The mechanical properties of the rabbit and human cornea. *J. Biomech.* **1986**, *19*, 847–853. [[CrossRef](#)]
4. Dyrland, T.F.; Poulsen, E.T.; Scavenius, C.; Nikolajsen, C.L.; Thøgersen, I.B.; Vorum, H.; Enghild, J.J. Human Cornea Proteome: Identification and Quantitation of the Proteins of the Three Main Layers Including Epithelium, Stroma, and Endothelium. *J. Proteome Res.* **2012**, *11*, 4231–4239. [[CrossRef](#)] [[PubMed](#)]
5. Fu, R.; Klinngam, W.; Heur, M.; Edman, M.C.; Hamm-Alvarez, S.F. Tear Proteases and Protease Inhibitors: Potential Biomarkers and Disease Drivers in Ocular Surface Disease. *Eye Contact Lens* **2020**, *46*, S70–S83. [[CrossRef](#)]
6. Kuo, M.-T.; Fang, P.-C.; Chao, T.-L.; Chen, A.; Lai, Y.-H.; Huang, Y.-T.; Tseng, C.-Y. Tear Proteomics Approach to Monitoring Sjögren Syndrome or Dry Eye Disease. *Int. J. Mol. Sci.* **2019**, *20*, 1932. [[CrossRef](#)]

7. Choi, S.-I.; Kim, T.-I.; Kim, K.S.; Kim, B.-Y.; Ahn, S.-Y.; Cho, H.-J.; Lee, H.K.; Kim, E.K. Decreased Catalase Expression and Increased Susceptibility to Oxidative Stress in Primary Cultured Corneal Fibroblasts from Patients with Granular Corneal Dystrophy Type II. *Am. J. Pathol.* **2009**, *175*, 248–261. [\[CrossRef\]](#) [\[PubMed\]](#)
8. Hohenstein-Blaul, N.V.T.U.; Kunst, S.; Pfeiffer, N.; Grus, F.H. Biomarkers for glaucoma: From the lab to the clinic. *Eye* **2017**, *31*, 225–231. [\[CrossRef\]](#)
9. Lauwen, S.; De Jong, E.K.; Lefeber, D.J.; Hollander, A.I.D. Omics Biomarkers in Ophthalmology. *Investig. Ophthalmology Vis. Sci.* **2017**, *58*, Bio88–Bio98. [\[CrossRef\]](#)
10. Klintworth, G.K. Corneal dystrophies. *Orphanet J. Rare Dis.* **2009**, *4*, 7–38. [\[CrossRef\]](#)
11. Aldave, A.J.; Sonmez, B.; Forstot, S.L.; Rayner, S.A.; Yellore, V.S.; Glasgow, B.J. A Clinical and Histopathologic Examination of Accelerated TGFBIp Deposition After LASIK in Combined Granular-Lattice Corneal Dystrophy. *Am. J. Ophthalmol.* **2007**, *143*, 416–419. [\[CrossRef\]](#)
12. Skonier, J.; Neubauer, M.; Madisen, L.; Bennett, K.; Plowman, G.D.; Purchio, A. cDNA Cloning and Sequence Analysis of β ig-h3, a Novel Gene Induced in a Human Adenocarcinoma Cell Line after Treatment with Transforming Growth Factor- β . *DNA Cell Biol.* **1992**, *11*, 511–522. [\[CrossRef\]](#) [\[PubMed\]](#)
13. Klintworth, G.K. The molecular genetics of the corneal dystrophies—Current status. *Front. Biosci.* **2003**, *8*, d687–d713. [\[CrossRef\]](#)
14. Klintworth, G.K.; Valnickova, Z.; Enghild, J.J. Accumulation of beta ig-h3 gene product in corneas with granular dystrophy. *Am. J. Pathol.* **1998**, *152*, 743–748. [\[PubMed\]](#)
15. Korvatska, E.; Henry, H.; Mashima, Y.; Yamada, M.; Bachmann, C.; Munier, F.L.; Schorderet, D.F. Amyloid and Non-amyloid Forms of 5q31-linked Corneal Dystrophy Resulting from Kerato-epithelin Mutations at Arg-124 Are Associated with Abnormal Turnover of the Protein. *J. Biol. Chem.* **2000**, *275*, 11465–11469. [\[CrossRef\]](#) [\[PubMed\]](#)
16. Karring, H.; Runager, K.; Valnickova, Z.; Thøgersen, I.B.; Møller-Pedersen, T.; Klintworth, G.K.; Enghild, J.J. Differential expression and processing of transforming growth factor beta induced protein (TGFBIp) in the normal human cornea during postnatal development and aging. *Exp. Eye Res.* **2010**, *90*, 57–62. [\[CrossRef\]](#) [\[PubMed\]](#)
17. Escribano, J. cDNA from human ocular ciliary epithelium homologous to beta ig-h3 is preferentially expressed as an extracellular protein in the corneal epithelium. *J. Cell. Phys.* **1994**, *160*, 511–521. [\[CrossRef\]](#)
18. Andersen, R.B.; Karring, H.; Møller-Pedersen, T.; Valnickova, Z.; Thøgersen, I.B.; Hedegaard, C.J.; Kristensen, T.; Klintworth, G.K.; Enghild, J.J. Purification and Structural Characterization of Transforming Growth Factor Beta Induced Protein (TGFBIp) from Porcine and Human Corneas. *Biochemistry* **2004**, *43*, 16374–16384. [\[CrossRef\]](#)
19. Lukassen, M.V.; Scavenius, C.; Thøgersen, I.B.; Enghild, J.J. Disulfide Bond Pattern of Transforming Growth Factor beta-Induced Protein. *Biochemistry* **2016**, *55*, 5610–5621. [\[CrossRef\]](#) [\[PubMed\]](#)
20. Kheir, V.; Cortés-González, V.; Zenteno, J.C.; Schorderet, D.F. Mutation update: TGFBI pathogenic and likely pathogenic variants in corneal dystrophies. *Hum. Mutat.* **2019**, *40*, 675–693. [\[CrossRef\]](#)
21. Lakshminarayanan, R.; Vithana, E.N.; Chai, S.-M.; Chaurasia, S.S.; Saraswathi, P.; Venkatraman, A.; Rojare, C.; Venkataraman, D.; Tan, D.; Aung, T. A novel mutation in transforming growth factor-beta induced protein (TGFBIp) reveals secondary structure perturbation in lattice corneal dystrophy. *Br. J. Ophthalmol.* **2011**, *95*, 1457–1462. [\[CrossRef\]](#) [\[PubMed\]](#)
22. Karring, H.; Runager, K.; Thøgersen, I.B.; Klintworth, G.K.; Højrup, P.; Enghild, J.J. Composition and proteolytic processing of corneal deposits associated with mutations in the TGFBI gene. *Exp. Eye Res.* **2012**, *96*, 163–170. [\[CrossRef\]](#)
23. Poulsen, E.T.; Nielsen, N.S.; Jensen, M.M.; Nielsen, E.; Hjortdal, J.; Kim, E.K.; Enghild, J.J. LASIK surgery of granular corneal dystrophy type 2 patients leads to accumulation and differential pro-teolytic processing of transforming growth factor beta-induced protein (TGFBIp). *Proteomics* **2016**, *16*, 539–543. [\[CrossRef\]](#)
24. Courtney, D.G.; Poulsen, E.T.; Kennedy, S.; Moore, J.E.; Atkinson, S.D.; Maurizi, E.; Nesbit, M.A.; Moore, C.B.T.; Enghild, J.J. Protein Composition of TGFBI-R124C- and TGFBI-R555W- Associated Aggregates Suggests Multiple Mechanisms Leading to Lattice and Granular Corneal Dystrophy. *Investig. Ophthalmology Vis. Sci.* **2015**, *56*, 4653. [\[CrossRef\]](#)
25. Venkatraman, A.; Dutta, B.; Murugan, E.; Piliang, H.; Lakshminarayanan, R.; Yee, A.C.S.; Pervushin, K.V.; Sze, S.K.; Mehta, J.S. Proteomic Analysis of Amyloid Corneal Aggregates from TGFBI-H626R Lattice Corneal Dystrophy Patient Implicates Serine-Protease HTRA1 in Mutation-Specific Pathogenesis of TGFBIp. *J. Proteome Res.* **2017**, *16*, 2899–2913. [\[CrossRef\]](#) [\[PubMed\]](#)
26. Poulsen, E.T.; Runager, K.; Risør, M.W.; Dyrland, T.F.; Scavenius, C.; Karring, H.; Praetorius, J.; Vorum, H.; Otzen, D.E.; Klintworth, G.K.; et al. Comparison of two phenotypically distinct lattice corneal dystrophies caused by mutations in the trans-forming growth factor beta induced (TGFBI) gene. *Proteom. Clin. Appl.* **2014**, *8*, 168–177. [\[CrossRef\]](#)
27. Karring, H.; Poulsen, E.T.; Runager, K.; Thøgersen, I.B.; Klintworth, G.K.; Højrup, P.; Enghild, J.J. Serine protease HtrA1 accumulates in corneal transforming growth factor beta induced protein (TGFBIp) amyloid deposits. *Mol. Vis.* **2013**, *19*, 861–876.
28. Berggård, T.; Linse, S.; James, P. Methods for the detection and analysis of protein–protein interactions. *Proteomics* **2007**, *7*, 2833–2842. [\[CrossRef\]](#)
29. Rao, V.S.; Srinivas, K.; Sujini, G.N.; Kumar, G.N.S. Protein-Protein Interaction Detection: Methods and Analysis. *Int. J. Proteom.* **2014**, *2014*, 1–12. [\[CrossRef\]](#) [\[PubMed\]](#)
30. Caprioli, R.M.; Farmer, T.B.; Gile, J. Molecular Imaging of Biological Samples: Localization of Peptides and Proteins Using MALDI-TOF MS. *Anal. Chem.* **1997**, *69*, 4751–4760. [\[CrossRef\]](#)
31. Schwamborn, K. Imaging mass spectrometry in biomarker discovery and validation. *J. Proteom.* **2012**, *75*, 4990–4998. [\[CrossRef\]](#) [\[PubMed\]](#)

32. Schwamborn, K.; Kriegsmann, M.; Weichert, W. MALDI imaging mass spectrometry—From bench to bedside. *Biochim. Biophys. Acta* **2017**, *1865*, 776–783. [[CrossRef](#)]
33. Venkatraman, A.; Hochart, G.; Bonnel, D.; Stauber, J.; Shimmura, S.; Rajamani, L.; Pervushin, K.; Mehta, J.S.; Anandalakshmi, V.; Lakshminaryanan, R. Matrix-Assisted Laser Desorption Ionization Mass Spectrometry Imaging of Key Proteins in Corneal Samples from Lattice Dystrophy Patients with TGFBI -H626R and TGFBI -R124C Mutations. *Proteom. Clin. Appl.* **2019**, *13*, e1800053. [[CrossRef](#)] [[PubMed](#)]
34. Yamazoe, K.; Yoshida, S.; Yasuda, M.; Hatou, S.; Inagaki, E.; Ogawa, Y.; Tsubota, K.; Shimmura, S. Development of a Transgenic Mouse with R124H Human TGFBI Mutation Associated with Granular Corneal Dystrophy Type 2. *PLoS ONE* **2015**, *10*, e0133397. [[CrossRef](#)] [[PubMed](#)]
35. Gessel, M.M.; Spraggins, J.; Voziyan, P.; Hudson, B.; Caprioli, R.M. Decellularization of intact tissue enables MALDI imaging mass spectrometry analysis of the extracellular matrix. *J. Mass Spectrom.* **2015**, *50*, 1288–1293. [[CrossRef](#)] [[PubMed](#)]
36. Poulsen, E.T.; Runager, K.; Nielsen, N.S.; Lukassen, M.V.; Thomsen, K.; Snider, P.; Simmons, O.; Vorum, H.; Conway, S.J.; Enghild, J.J. Proteomic profiling of TGFBI-null mouse corneas reveals only minor changes in matrix composition supportive of TGFBI knockdown as therapy against TGFBI-linked corneal dystrophies. *FEBS J.* **2018**, *285*, 101–114. [[CrossRef](#)] [[PubMed](#)]
37. Poulsen, E.T.; Nielsen, N.S.; Scavenius, C.; Mogensen, E.H.; Risør, M.W.; Runager, K.; Lukassen, M.V.; Rasmussen, C.B.; Christiansen, G.; Richner, M.; et al. The serine protease HtrA1 cleaves misfolded transforming growth factor beta-induced protein (TGFBIp) and induces amyloid formation. *J. Biol. Chem.* **2019**, *294*, 11817–11828. [[CrossRef](#)]
38. Anandalakshmi, V.; Murugan, E.; Leng, E.G.T.; Ting, L.W.; Chaurasia, S.S.; Yamazaki, T.; Nagashima, T.; George, B.L.; Peh, G.S.L.; Pervushin, K.; et al. Effect of position-specific single-point mutations and biophysical characterization of amyloidogenic peptide fragments identified from lattice corneal dystrophy patients. *Biochem. J.* **2017**, *474*, 1705–1725. [[CrossRef](#)]
39. Sørensen, C.S.; Runager, K.; Scavenius, C.; Jensen, M.M.; Nielsen, N.S.; Christiansen, G.; Petersen, S.V.; Karring, H.; Sanggaard, K.W.; Enghild, J.J. Fibril Core of Transforming Growth Factor Beta-Induced Protein (TGFBIp) Facilitates Aggregation of Corneal TGFBIp. *Biochemistry* **2015**, *54*, 2943–2956. [[CrossRef](#)]
40. Underhaug, J.; Koldsø, H.; Runager, K.; Nielsen, J.T.; Sørensen, C.S.; Kristensen, T.; Otzen, D.E.; Malmendal, A.; Schiøtt, B.; Enghild, J.J.; et al. Mutation in transforming growth factor beta induced protein associated with granular corneal dystrophy type 1 reduces the proteolytic susceptibility through local structural stabilization. *Biochim Biophys Acta.* **2013**, *1834*, 2812–2822. [[CrossRef](#)]
41. Koldso, H.; Andersen, O.J.; Nikolajsen, C.L.; Scavenius, C.; Sørensen, C.S.; Underhaug, J.; Runager, K.; Nielsen, N.C.; Enghild, J.J.; Schiøtt, B. Early Events in the Amyloid Formation of the A546T Mutant of Transforming Growth Factor β -Induced Protein in Corneal Dystrophies Compared to the Nonfibrillating R555W and R555Q Mutants. *Biochemistry* **2015**, *54*, 5546–5556. [[CrossRef](#)] [[PubMed](#)]
42. Hou, Y.C.; Hu, F.R.; Chen, M.S. An autosomal dominant granular corneal dystrophy family associated with R555W mutation in the BIGH3 gene. *J. Formos. Med. Assoc.* **2003**, *102*, 117–120. (In Chinese) [[PubMed](#)]
43. Romero, P.; Moraga, M.; Herrera, L. Different phenotypes of lattice corneal dystrophy type I in patients with 417C > T (R124C) and 1762A > G (H572R) mutations in TGFBI (BIGH3). *Mol. Vis.* **2010**, *16*, 1601–1609. [[PubMed](#)]
44. Morishige, N.; Chikama, T.-I.; Ishimura, Y.; Nishida, T.; Takahashi, M.; Mashima, Y. Unusual Phenotype of an Individual with the R124C Mutation in the TGFBI Gene. *Arch. Ophthalmol.* **2004**, *122*, 1224. [[CrossRef](#)] [[PubMed](#)]